

# Supporting Information

Saint-Geniez et al. 10.1073/pnas.0905010106

## SI Materials and Methods

**Immunohistochemistry.** Whole embryos or enucleated eyes were fixed overnight in 10% buffered formalin, Histochoice MB (Amresco), or 4% paraformaldehyde in PBS and prepared for paraffin or cryosections. For histology, paraffin sections of E13.5 wt and VEGF188/188 embryo were dewaxed, rehydrated, and stained with hematoxylin and periodic acid Schiff. For immunohistochemistry, rehydrated paraffin sections were pretreated by boiling in citrate buffer, pH 6.0, and incubated with 1% H<sub>2</sub>O<sub>2</sub> in methanol for 10 min to block endogenous peroxidase activity. Antibodies were visualized using avidin-biotin-horseradish peroxidase and DAB substrate (Vector ABC kit; Vector Laboratories) or by fluorescent immunodetection using Cy3- or FITC-conjugated matching secondary antibody (Jackson ImmunoResearch Laboratories) and DAPI for cell nucleus labeling. For each experiment, a section was incubated with isotope-matched IgG as a negative control. Primary antibodies included rat anti-endomucin (1), rabbit anti-mouse  $\beta$ -catenin (Upstate), and rabbit anti-mouse occludin (Invitrogen). Some RPE flat-mounted preparations were co-stained for F-actin using TRIC-phalloidin (1:200; Molecular Probes).

**Histology and Electron Microscopy.** wt and VEGF 188/188 mice were anesthetized with ketamine and xylazine and fixed via aortic perfusion with 10 mL sodium cacodylate buffer 0.2 M, pH 7.4, followed by 10 mL half-strength Karnovsky's fixative (formaldehyde/glutaraldehyde, 2.5% each in 0.1 M sodium cacodylate buffer, pH 7.4; both from Electron Microscopy Sciences). The eyes were dissected out, and the anterior segment (cornea and lens) removed. The eyecups were postfixed in 2% osmium tetroxide. The tissues were dehydrated and embedded in Embed 812. Sections for light microscopy were cut at 1 or 2  $\mu$ m and stained with *p*-phenylenediamine or Richardson's stain (methylene blue and azur II). Ultrathin sections were treated with uranyl acetate and visualized using a Phillips 410 transmission electron microscope (Eindhoven). For measurement of BrM thickness, electron micrographs were taken at 21,000 $\times$ . At least 20 photographs per sample were used for the quantification. Three measurements of the BrM thickness were made per photograph (for a total of over 60 measurements) and averaged using ImageJ software (<http://rsb.info.nih.gov/ij>).

**ERG Recordings.** The ERGs of VEGF188/188 and wt mice were assessed using a UTAS-E3000 recording system (LKC Technologies) ( $n = 4$ ). Mice were dark-adapted overnight and anesthetized with a mixture of ketamine/xylazine (120 mg/kg and 10 mg/kg, respectively). Their pupils were dilated with 1% tropicamide, 1.5% cyclopentolate. After pupil dilatation with 1% tropicamide, 1.5% cyclopentolate, each mouse was placed in front of a Ganzfeld bowl (UTAS3000; LKC Technologies). The active electrode, a gold wire loop, was placed on the cornea, the reference electrode was placed on the head, and the ground electrode was placed on the back. ERG responses to a series of increasing-intensity light flashes:  $\pm 0$ , +10, and +20 dB were

averaged over 10 separate flashes per light intensity. The a-wave amplitude was measured from the baseline to the trough of the first negative wave; the b-wave amplitude was measured from the trough of the a-wave to the peak of the first positive wave or, if the a-wave is absent, from baseline to the peak of the first positive wave.

**Retina Fundus.** Fundus photographs were taken with a Topcon/Imagenet system (Topcon Medical System) with a preset 20D lens apposed to the fundus camera.

**Western Blot Analysis and Immunoprecipitation.** Eyes from wt and VEGF188/188 mice were removed under the dissecting microscope. The retina and RPE-choroid tissue were separated and homogenized in lysis buffer (Cell Signaling). Each sample represented one mouse. Protein concentration was quantified using a BCA assay (Bio-Rad Laboratories). For Western blot analysis, identical amount of protein was separated by SDS-PAGE under reducing condition, and transferred to Immobilon-P membrane (Millipore). Membranes were incubated overnight at 4  $^{\circ}$ C with  $\beta$ -catenin (1:500; Upstate) or actin (1:1,000; Santa Cruz Biotechnologies) antibodies. To quantify the level of VEGFR2 phosphorylation, membranes were incubated with a polyclonal anti-Y1214-VEGFR2 antibody (1:500; Biosource). Total VEGFR2 was detected by stripping the membranes by incubation for 15–30 min in 6.25 mM Tris-HCl, pH 6.8, 2% SDS, and 100 mM  $\beta$ -mercaptoethanol at 50  $^{\circ}$ C and reprobing with a polyclonal VEGFR2 antibody (1:1,000; Cell Signaling). Changes in occludin/ZO1 association were analyzed by immunoprecipitation according to the method of Collins et al. (see main text, Reference 28). Occludin was immunoprecipitated overnight at 4  $^{\circ}$ C from 60  $\mu$ g RPE-choroid lysates with 1.75  $\mu$ g polyclonal rabbit anti-mouse occludin antibody (Zymed). Immunoprecipitate complexes were analyzed by SDS-PAGE with a polyclonal anti-mouse ZO1 antibody (1:1,000; Zymed). Scanning densitometry was performed with image-analysis software (ImageJ).

**TUNEL Assay.** Apoptotic cells were detected in retinal cryosections using the In Situ Cell Death Detection TMR red kit (Roche Diagnostic) following the manufacturer's instructions with some modifications. Briefly, eye sections were permeabilized for 5 min in cold PBS containing 0.2% Tween-20. Sections were then incubated at 37  $^{\circ}$ C in TUNEL reaction mix containing biotinylated nucleotides and terminal deoxynucleotidyl transferase (TdT). DNase treatment was performed as a positive control, and incubation without TdT enzyme was conducted as a negative control.

**Statistical Analysis.** Values are expressed as mean  $\pm$  SEM (unless specified), and statistical analysis was performed using an unpaired Student *t*-test (\*\*\*,  $P < 0.001$ ; \*\*,  $P < 0.01$ ; \*,  $P < 0.05$ ; ns,  $P > 0.05$ ).

1. Brachtendorf G, et al. (2001) Early expression of endomucin on endothelium of the mouse embryo and on putative hematopoietic clusters in the dorsal aorta. *Dev Dyn* 222:410–419.

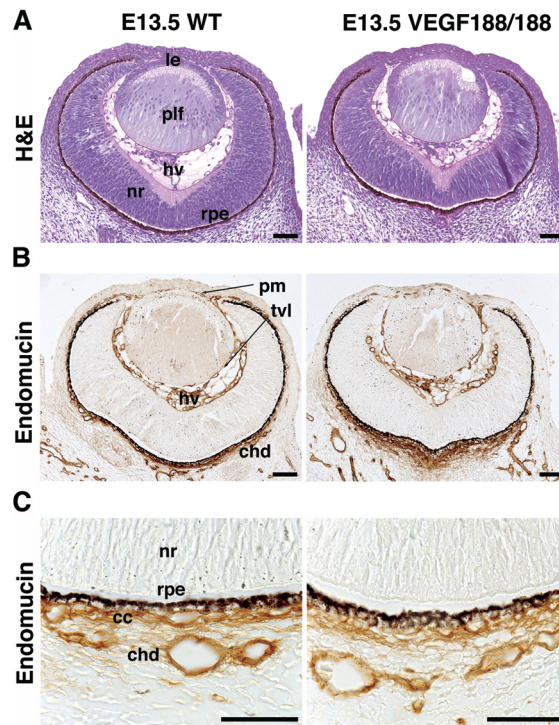


**Fig. S1.** Normal eye development in VEGF188/188 mice. (A–C) Paraffin sections of E13.5 wt (left panel) and VEGF188/188 (right panel) mice were stained with hematoxylin-periodic acid-Schiff or with the endothelial-specific marker, endomucin. At E13.5, eyes from VEGF188/188 display normal histology (top panel). (B) The ocular vascular beds, hyaloid vessels, and choroids of VEGF188/188 mice stained by endomucin appeared normal. (C) Higher magnification of the back of the eye showed normal RPE differentiation and choroidal vessel organization. Note the characteristic association between the CC and the primitive RPE. (Scale bar, 50  $\mu$ m.) nr, neuronal retina; chd, choroid; cc, choriocapillaris; le, lens epithelium; plf, primary lens fiber; hv, hyaloid vessels; pm, pupillary membrane; tvl, tunica vasculosa lentis.

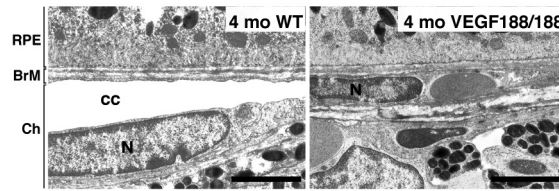


**Fig. S2.** Normal ultrastructure of the outer retina in young VEGF188/188 mice. One-micrometer-thin epon sections of retinas from 4-month-old wt (left panel) and VEGF188/188 (right panel) mice were visualized by TEM. No changes in the ultrastructure of the RPE-choroid complex were observed in VEGF188/188 mice. Thickness and organization of the BrM appeared normal. (Scale bar, 2.5  $\mu$ m.) rpe, retinal pigmented epithelium; BrM, Bruch's membrane; Ch, choroid; N, endothelial cell nuclei; CC, choriocapillaris lumen.

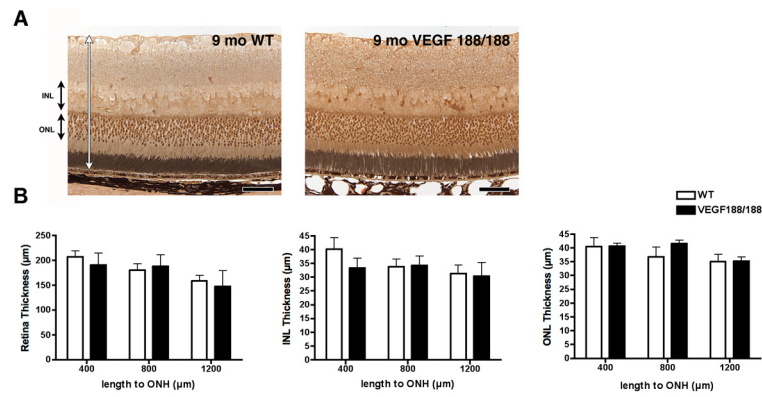


**Fig. S3.** Normal retinal architecture in aged VEGF188/188 mice. (A) Analysis of semithin epon sections 9-month-old VEGF188/188 and wt retinas showed no architectural anomalies. (B) Quantification of the total retina, INL, and ONL thickness revealed no significant change in 8- to 10-month-old VEGF188/188 mice compared to aged-matched wt ( $n = 3$ ). INL, inner nuclear layer; ONL, outer nuclear layer. (Scale bar, 20  $\mu\text{m}$ .)

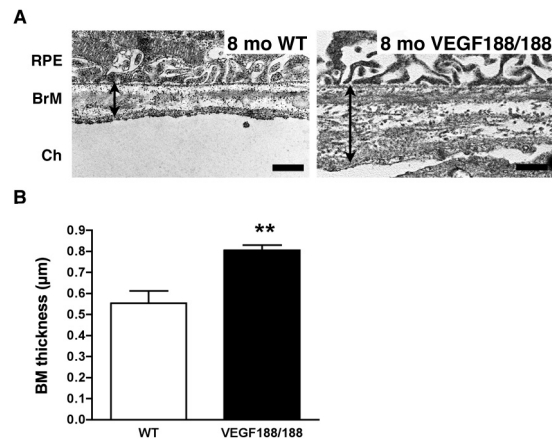


**Fig. 54.** Increased BrM thickness in aged VEGF188/188 mice. (A) Electron micrograph of the outer retina of 8-month-old animals revealed a significant thickening of the BrM of the VEGF188/188 mice compared to wt (as shown by double-headed arrows). (B) The mean thickness of BrM in the eyes of 8- to 12-month-old VEGF188/188 mice was increased 5% over the wt control ( $0.81 \pm 0.02 \mu\text{m}$  for VEGF188/188 compared to  $0.55 \pm 0.06 \mu\text{m}$  for wt,  $n = 3$ ,  $P = 0.0022$ ). (Scale bar, 500 nm.) RPE, retinal pigmented epithelium; BrM, Bruch's membrane; Ch, choroidal vessel.

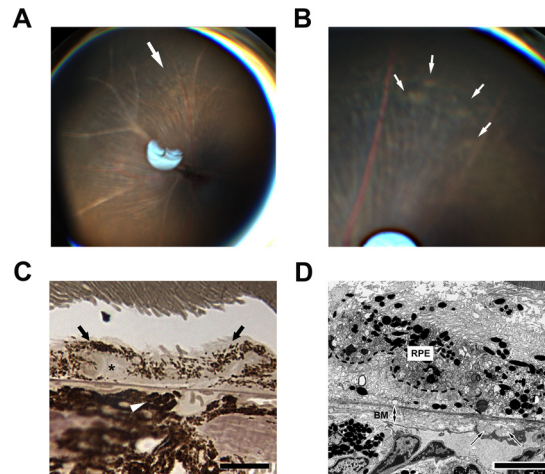


**Fig. 55.** Fundus anomalies in 14-month-old VEGF188/188 mice. (A) Subretinal lesions and hypopigmented RPE in the mid-periphery of a 14-month-old VEGF188/188 mouse (arrow). (B) Higher magnification showing drusen-like yellowish deposits (arrows). (C) Thin section through one of these drusen-like lesions in a 12-month-old VEGF188/188 mouse showing folding of the RPE layer with swollen and degenerative cells (black arrows) above some large subretinal deposit (asterisk). Note that the photoreceptors were detached from the RPE; no detachment was detected in normal regions of the retina. Beneath the lesion, the choroid and sclera organization appeared abnormal, with melanocytes invading the choroidal space (white arrowhead). (D) Ultrastructure of the lesion showing clumped RPE cells and thick basal deposit containing laminar and membranous material (outlined by dotted line). Beneath the lesion, BrM is thickened (double-headed arrow) with debris-filled vacuoles (arrows). [Scale bar, 20  $\mu\text{m}$  (C); 5  $\mu\text{m}$  (D).]

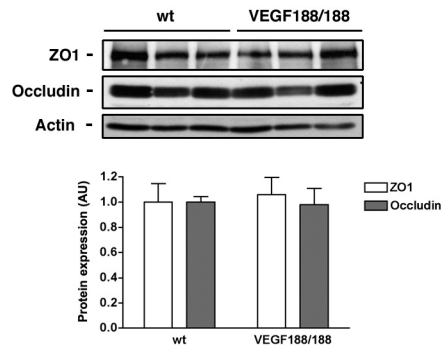


**Fig. S6.** ZO1 and occludin protein levels in 16-month-old VEGF188/188 mice. ZO1 and occludin protein levels were quantified by Western blot of choroid-RPE samples from 16-month-old VEGF188/188 and wt mice ( $n = 6$  for ZO1 and  $n = 3$  for occludin). Densitometric analysis showed no changes in ZO1 and occludin expression in VEGF188/188 compared to wt ( $P = 0.7723$  for ZO1 and  $P = 0.8934$  for occludin).

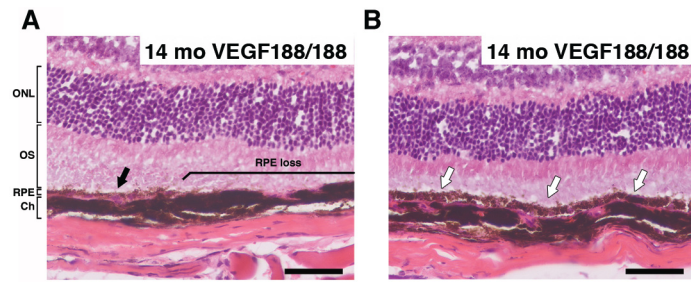


**Fig. 57.** RPE atrophy in aged VEGF188/188 mice. (A) Histological section of 14-month-old VEGF188/188 eye showing a large zone denuded of RPE cell adjoining a region of abnormal and thinned RPE cells (black arrow). Note that at the site of RPE atrophy, the photoreceptor outer segments are directly abutting to the Bruch's membrane. (B) Picture from the same sample taken away from RPE lesions showing normal outer retina organization (white arrows). (Scale bar, 50  $\mu$ m.)



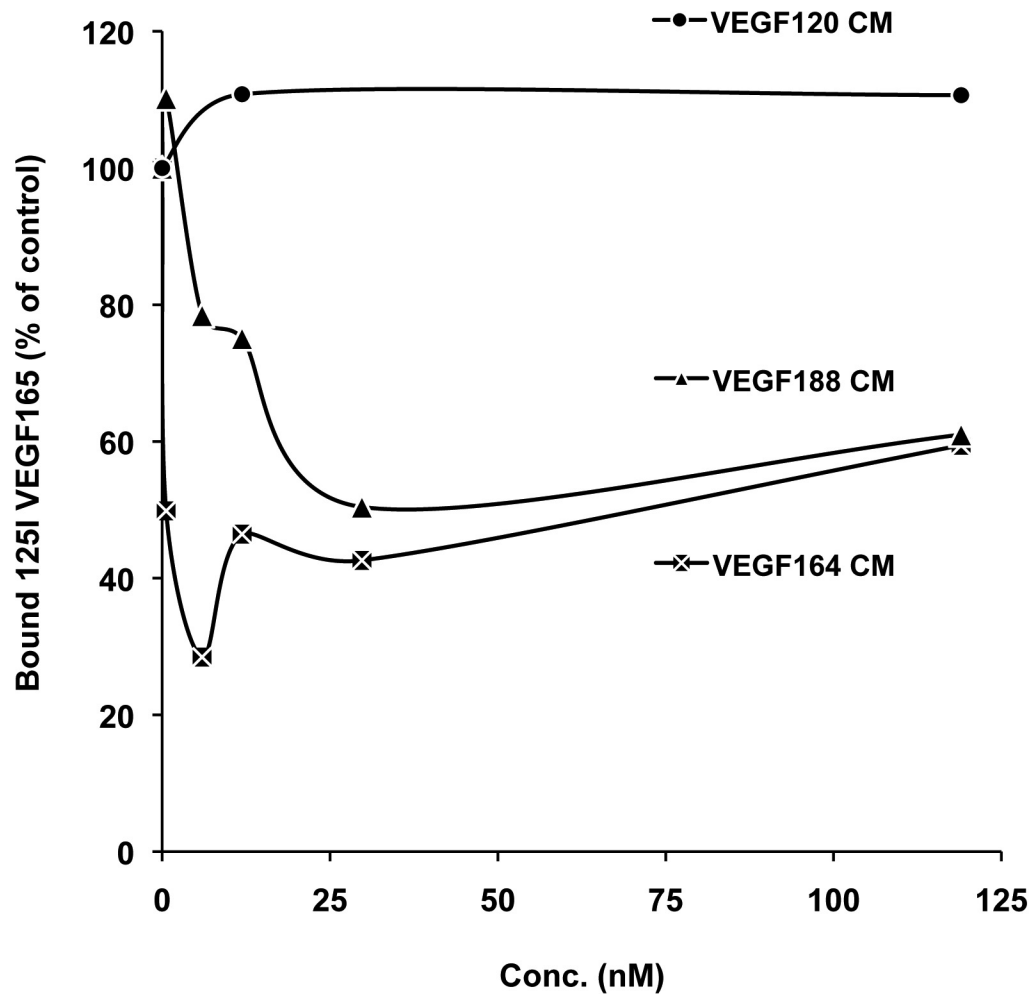


**Fig. 58.** Inhibition of  $^{125}\text{I}$  VEGF<sub>165</sub> binding to porcine aortal endothelial cells stably transfected with Neuropilin-1 (PAE-NRP1) by conditioned media containing murine VEGF120, VEGF164, or VEGF188. VEGF isoforms (VEGF188, 164, and 120) were produced by transient transfection of HEK293. Three days later, the conditioned medium (CM) was collected, filtered, and concentrated using a Centricon plus 70 (Millipore). The final concentration of VEGF isoform was quantified by ELISA (R&D Systems). For the competition-binding experiments, PAE-NRP1 cells were incubated with  $^{125}\text{I}$ -VEGF165 (5 ng/mL) in binding buffer with increasing concentrations of cold VEGF isoforms in CM for 1 h at 4 °C. The results are reported as a percent of the control ( $^{125}\text{I}$  VEGF165 alone). The experiment was conducted in duplicated. As expected, VEGF 120, which does not bind Neuropilins, was not able to inhibit  $^{125}\text{I}$ -VEGF165 binding to Neuropilin-1. Both the conditioned media containing VEGF188 and VEGF164, showed a strong displacement of  $^{125}\text{I}$ -VEGF165 at the concentrations analyzed, which confirm that VEGF188 is able to bind NP1 as suggested by the presence of the Neuropilin-1 binding site.